



**LUT**  
Lappeenranta  
University of Technology

## **Enzymatically hydrolyzed and agitated biomass suspensions: experimental determination of fiber size distributions and filtration characteristics**

Kinnarinen Teemu, Koironen Tuomas, Häkkinen Antti, Louhi-Kultanen Marjatta

This is a Final draft version of a publication

published by Editura Academiei Romane

in Cellulose Chemistry and Technology

**DOI:**

**Copyright of the original publication:** © Editura Academiei Romane 2014

**Please cite the publication as follows:**

Kinnarinen, T., Koironen, T., Häkkinen, A., Louhi-Kultanen, M., Enzymatically hydrolyzed and agitated biomass suspensions: experimental determination of fiber size distributions and filtration characteristics, Cellulose Chemistry and Technology, 2014, 48 (3-4): 299-311. [http://www.cellulosechemtechnol.ro/pdf/CCT3-4\(2014\)/p.299-311.pdf](http://www.cellulosechemtechnol.ro/pdf/CCT3-4(2014)/p.299-311.pdf)

**This is a parallel published version of an original publication.  
This version can differ from the original published article.**

# ENZYMATICALLY HYDROLYZED AND AGITATED BIOMASS SUSPENSIONS: EXPERIMENTAL DETERMINATION OF FIBER SIZE DISTRIBUTIONS AND FILTRATION CHARACTERISTICS

TEEMU KINNARINEN\*, TUOMAS KOIRANEN,  
ANTTI HÄKKINEN and MARJATTA LOUHI-KULTANEN

*Laboratory of Separation Technology, Lappeenranta University of Technology,*

*P.O. Box 20, FI-53851 Lappeenranta, Finland*

*\*Corresponding author tel: +358 40 562 1398, e-mail: [teemu.kinnarinen@lut.fi](mailto:teemu.kinnarinen@lut.fi)*

## ABSTRACT

Separation processes in general present a significant challenge in the production of bioethanol from lignocellulosic materials. Solid-liquid separation, prior to the concentration of ethanol (for instance, by distillation), is often essential and upstream process conditions may determine how effectively this separation can be performed. In this experimental study, properties of a lignocellulosic solid residue, generated through the enzymatic hydrolysis of biomass, and solid-liquid separations after the hydrolysis stage were studied, focusing on the fiber and particle size distribution (FSD and PSD) of the solids. During the course of enzymatic hydrolysis, fiber and particle size distributions of the biomass during and after enzymatic hydrolysis were measured using a fiber tester and a laser diffraction analyzer, respectively, in order to quantify the effect of enzymatic saccharification on the size distribution of the suspended solids. The main target, however, was to investigate the filtration properties of hydrolyzed and agitated suspensions using a pressure filter. The particle size distributions of the filtered samples were measured with the laser diffraction analyzer. Even though the filtration properties were strongly influenced by agitation, the effect on particle size distributions was found to be much smaller. During enzymatic hydrolysis, the most significant reduction in the size of the solids took place rapidly after the cellulase addition. The width of the fibers was not observed to decrease during the hydrolysis stage.

**Keywords:** Enzymatic hydrolysis, Fiber size, Particle size, Mixing, Agitation, Filtration

## INTRODUCTION

Enzymatic hydrolysis for cleaving cellulose to sugars may be one of the key enabling technologies for the production of bioethanol from lignocellulosic raw materials that are sustainably available. Such raw materials include the waste fractions of agriculture, forestry, the pulp and paper industry, as well as waste paper and cardboard collected from municipal and industrial sources. After six decades of development, accelerated by the energy crisis in the 1970s, commercially feasible enzymatic degradation of biomass is gradually becoming a reality.<sup>1</sup> A number of large pilot plants for producing ethanol from lignocellulosic biomass have recently been established, for instance, in Europe, Canada and the United States.<sup>2</sup> Lignocellulosic biomass is, however, typically highly resistant to enzymatic saccharification, which results in a high enzyme requirement and, consequently, limited applicability to many potential raw materials.

Regardless of the current technological problems related to the hydrolysis stage, paper and cardboard products have the potential to become an important source of fermentable sugars for the production of lignocellulosic ethanol. The use of waste fibre and papers has been recently studied by, amongst others, Kemppainen et al.<sup>3</sup> and Wang et al.<sup>4</sup> and, earlier, by Mandels et al.<sup>5</sup> and Walpot<sup>6</sup>. Cardboard waste is globally available and its structure is suitable for further processing. Recycling and incineration are the two most common ways of utilizing the material and energy content of cardboard waste. Unfortunately, the enzymatic hydrolysis of lignocellulose, including products of paper and pulp industry is challenging,<sup>7,8</sup> especially because of fiber hornification.<sup>9</sup> The effect of enzymatic hydrolysis on the fiber properties is not completely understood. Solid-liquid separation of enzymatically hydrolyzed lignocellulosic suspensions is another process step in which changes in the process can bring about unpredictable results.<sup>10</sup> As proposed in many previous studies on separate hydrolysis and fermentation (SHF), solid-liquid separation may be essential at various stages of the bioethanol process: after either pretreatment, hydrolysis, fermentation or after the ethanol recovery by distillation.<sup>11-15</sup> In any event, non-degraded fibers in the hydrolysate could have an adverse effect on fermentation and downstream separations.<sup>12</sup> In the case of lignocellulosic ethanol, the hydrolysis stage has been studied more extensively than the downstream separation processes. More attention has been previously paid to the solid-liquid separation of other difficult-to-filter suspensions, such as wastewater sludges. There are some similarities between biomass hydrolysates and wastewater sludges, including high cake compressibility<sup>16</sup>, difficult deliquoring of cakes with low fiber content,<sup>17</sup> and limited possibilities to increase the solids content of the cakes.

Several factors, either separately or together, determine the success of enzymatic hydrolysis. These factors include, for instance, crystallinity of cellulose,<sup>18-20</sup> and particle size of biomass.<sup>21-24</sup> The quality of the cellulosic biomass itself has an influence on enzymatic hydrolysis and, conversely, hydrolysis alters the physical properties and the chemical composition of the biomass. During enzymatic hydrolysis, properties such as the pore volume<sup>20</sup> and the average length<sup>23</sup> of cellulosic fibers may be reduced. Pulping, as well as enzymatic treatment,<sup>25</sup> may drastically change the morphology and properties of cellulose fibers.<sup>26,27,9</sup> The effect of mixing on enzymatic saccharification has been recently evaluated<sup>28,29</sup>, but its effect on separation performance is still unclear.

The topic of this article, the influence of enzymatic hydrolysis and mixing conditions on the fiber and particle size of a lignocellulosic biomass and the filtration characteristic of the resulting suspensions, is a continuation of the authors' previous work<sup>30</sup>. In this previous paper, it was stated that both the extent of hydrolysis and mixing conditions affected solid-liquid separation characteristics. The influence of mixing conditions on the yield of hydrolysis has been investigated in several studies, but the results vary, depending on factors such as the substrate quality and quantity, enzymes used, as well as reaction time.<sup>31</sup> The purpose of this article is to show how important a role mixing plays with respect to the solid-liquid separation of lignocellulosic hydrolysates and how it affects the particle size. The effect of the degree of conversion is eliminated by using the same hydrolyzed suspension in all experiments. Furthermore, measurement of fiber and particle size distributions, carried out with two different instruments, a fiber tester and a laser diffraction particle size analyzer, during the enzymatic hydrolysis, will help to understand better how the fiber size is reduced during enzymatic saccharification and how it correlates with the resulting filtration properties.

## EXPERIMENTAL

### Description of the process

A sample of air dry old corrugated cardboard, collected from Finland and shredded prior to transportation to the laboratory, was first milled, using a hammer mill. The aim of milling was to reduce the initial particle size to a range measurable with the particle and fiber size analyzers and to enable rapid wetting of fibers. The device was equipped with a screening system, in which a screen with a mesh size of 2 mm was used. After forming the solid-liquid suspensions for the experiments, and thus after complete wetting of the material, the size distributions were measured.

Enzymatic hydrolysis, of duration 72 hours, was performed using the milled cardboard waste, described above, as the model biomass. The enzymes were commercial cellulase and hemicellulase products, Cellic CTec2 and Cellic HTec (Novozymes, Denmark). The enzyme dosages were 150 mL of CTec per kilogram of cellulose and 30 mL of HTec per kilogram of dry raw material. The FPU activity for the cellulase product has been reported to be approximately 120-150 FPU/mL.<sup>32,33</sup> The cellulose and lignin contents of the cardboard waste, previously described by Kinnarinen et al.<sup>10</sup> were 63 wt.% and 11.5 wt.%, respectively. The ash content of the raw material was 9.1 wt.%, obtained by dry oxidation at 575 °C (ASTM D3516–89(2006) standard). The hemicellulose content was therefore estimated to be approximately 15 wt.%.

After hydrolysis, there was a certain amount of non-hydrolyzed solid residue (cellulose, lignin, minerals, pigments and other impurities) in the suspension. The aim was to separate this residue from the monosaccharide-containing liquid using a laboratory-scale pressure filter. Filtration tests were performed both after the hydrolysis and after additional mixing. In most tests, the filtration pressure was 100 kPa (1 bar). In addition, in order to determine the compression properties of the filter cake produced, filtration tests were also performed at two further pressures (3.5 and 6 bar).

### Equipment and conditions

The hydrolysis experiments were carried out in a mixing device, which consisted of six mixing tanks ( $D_t = 110$  mm,  $h_t = 170$  mm), mixing elements with electric motors, and a temperature-controlled bath. The volume of the suspension prepared in each tank was 1.3 L. Because pH has an important role in the hydrolysis, the pH of each batch of suspension was slowly adjusted to 5.0 with 2.0 M sulfuric acid. The water bath was kept at a constant 46 °C ( $\pm 0.2$  °C) for 72 h, and the mixing speed was held constant during the hydrolysis. The solid content in all slurry batches was 10.0 wt.% and the rotation speed of each impeller was 40 rpm (0.67 1/s). Identical anchor-shaped (Fig. 1(a)) impellers ( $d_i = 97$  mm,  $h_i = 120$  mm) without baffles were employed in each batch to avoid mechanical reduction of particle size.

In this part of the study, any reduction of particle size of the model biomass during the hydrolysis stage was investigated and the suspension samples for the mixing experiments produced. The initial fiber and particle size distributions of the biomass are presented with the results in the Results and Discussion Section.

### Determination of particle sizes and sugar concentrations

For the fiber and particle size measurements and the determination of monosaccharides, nine samples were taken from each of the six tanks during the hydrolysis (after 1, 2, 3, 5, 8.5, 12, 24, 48 and 72 hours) and one sample prior to adding the enzymes. There was no reason for

more frequent sampling intervals during the first hours of hydrolysis, because the kinetics of enzymatic saccharification were out of the scope for this study. Six samples of equal volume (7 mL), intended for sugar determination, were combined, vacuum filtered through Whatman #42 filter paper to separate most solids, and finally filtered through a syringe filter (0.2  $\mu\text{m}$ ). For the fiber and particle size measurements, the samples were kept in a water bath at 100 °C for 10 minutes in order to stop the progress of hydrolysis.

The fiber size distributions were determined using a Lorentzen & Wettre fiber tester (Kista, Sweden). This instrument was capable of measuring both the length and width distribution of the fibers using an image analysis technique. The ranges for the measurable fiber length and width were 0.2-7.5 mm and 10-100  $\mu\text{m}$ , respectively. Objects smaller than 0.2 mm in length were regarded as fines and therefore excluded from the fiber size distributions. Premilling of the raw material was probably the main reason for the abundance of fibers shorter than 1 mm also in the original suspension. Fiber size measurement was performed 2-3 times for each sample.

The volumetric particle size distributions (PSD) were measured with a Beckman Coulter LS13320 laser diffraction analyzer. The Fraunhofer model of light scattering was selected as the calculation basis for the measurements. The size range of the particles that could be analyzed using this device was from 0.04 to approx. 2,000  $\mu\text{m}$ . Within this range, the particle size analyzer measured all solids, without the ability to distinguish between spherical and elongated particles. Each measurement was performed at least 6 times for each sample and the results were averaged. While it is probable that the particle size analysis, which is most suitable for spherical particles, cannot completely detect changes in the fiber size during the hydrolysis stage, it can be used for acquiring comparative data about the relative size of solid particles in the suspension that may affect both the hydrolysis rate and the subsequent solid-liquid separation processes. Only this technique was used for measuring the size of the solids after the mixing experiments, because the cut fibers and other fine solids in particular were expected to be responsible for the resistance to filtration.

A JEOL JSM-5800 scanning electron microscope (15 kV, 100 x magnification) was used for visual characterization of the fibers. The samples were first diluted with 10-fold volume of Millipore water, filtered through Whatman 42 filter paper to recover the fibers, and finally dried slowly at room temperature.

The two main monosaccharides, liberated from the polysaccharide matrix during hydrolysis, glucose and xylose, were determined by high performance liquid chromatography, HPLC (HP Agilent 1100), using a Varian Metacarb 87H column. The temperature during the elution was 60 °C and the eluent was 5 mM  $\text{H}_2\text{SO}_4$ , with a flow rate of 0.6 mL/min and an injection volume of 10  $\mu\text{L}$ . It is possible that small amounts of other monomeric sugars and cellobiose were also present in the hydrolysates, although they were not assayed in this case.

### **Mixing experiments**

After the hydrolysis, the slurry was mixed with two impellers: a Rushton blade turbine and a conventional propeller (Fig. 1(b-c)). The rotational diameter of both impellers was 70 mm. The distance of the impellers from the bottom of the mixing tanks was 15 mm. Baffles were installed in the tanks to increase turbulence and the potential for size reduction of the particles during mixing.

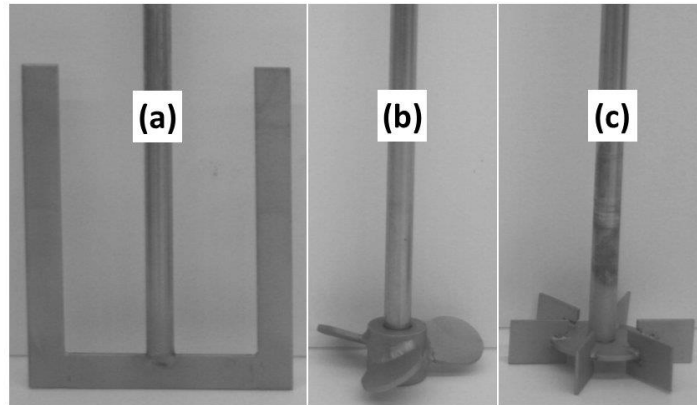


Figure 1: The mixing elements: The anchor used for agitation during the hydrolysis stage (a). The propeller (b) and the Rushton turbine (c) used in the filtration part of the study

In order to investigate the effect of mixing on the particle size and filtration properties of the slurry, three rotation speeds (100, 300, 500 rpm) were used. Filtration tests were performed prior to the additional mixing, after 0.5 hours, and finally after 4 h of mixing. The samples for the PSD measurement were taken at the same time as those for the filtration, and additionally after 2 hours of mixing. The experimental plan is shown in Table 1.

Table 1  
Mixing conditions for filtration experiments and particle size analysis

Test	Mixer type	Rotation speed (rpm)	Mixing time, filtration (h)	Mixing time, PSD measurement (h)
1	Rushton	100	0.5; 4	0.5; 2; 4
2	Rushton	300	0.5; 4	0.5; 2; 4
3	Rushton	500	0.5; 4	0.5; 2; 4
4	Propeller	100	0.5; 4	0.5; 2; 4
5	Propeller	300	0.5; 4	0.5; 2; 4
6	Propeller	500	0.5; 4	0.5; 2; 4

### Filtration experiments

Immediately after sampling, the solids were separated from the fresh and mixed hydrolysates by pressure filtration. Batches of 200 g were filtered at 23 °C using a laboratory-scale filter (Nutsche). The filter chamber was pressurized with nitrogen: the applied gas pressures were 1, 3.5 and 6 bar. A cellulosic disc (T1000, Pall Corporation) with a cut-off particle size of 24 µm was used as the filter medium. After 72 hours of hydrolysis, the ability of the cellulase present in the suspension to degrade cellulose was very limited, mainly due to the temperature which was far below the optimum, so there was no significant risk of degradation of the filter medium during the relatively short (2-15 min) filtration experiments. Additionally, each disc of filter medium was used only once. The thickness and the effective filtration area of the filter medium were 3.6 mm and 18.9 cm<sup>2</sup>, respectively. The estimated concentration of total suspended solids

in the slurry was 5.8 wt.%. The total solid contents in the filter cakes were typically approximately 30 wt.%, consisting of suspended (about 85 wt.% of the total) and dissolved solids (about 15 wt.% of the total).

All cakes were analyzed for the total solids (TS) concentration by drying them in a heating chamber at 105 °C until the weight was constant. The total dissolved solids (TDS) content in the filtrate was approximated using a Brix refractometer after filtering the filtrate sample through a syringe filter (0.2 µm nominal pore size). The TDS content in the filtrate was typically approximately 60 g/L.

### Calculations

The specific resistance of a filter cake,  $\alpha$ , can be determined from Eq. (1), derived from Darcy's basic filtration equation:

$$\frac{dt}{dV} = \frac{\alpha\mu c}{A^2 \Delta p} V + \frac{\mu R}{A \Delta p} \quad (1)$$

where  $t$  (s) is time,  $V$  (m<sup>3</sup>) is the filtrate volume,  $\alpha$  (m/kg) is the specific resistance of the filter cake,  $\mu$  (Pa s) is the dynamic viscosity and  $c$  (kg<sub>solids</sub>/m<sup>3</sup><sub>filtrate</sub>) is the filtration concentration that is defined as the mass of solid material in the filter cake per unit volume of filtrate collected (and is in turn related to the solidosity of the cake and the solids content of the slurry). The filtration pressure is  $\Delta p$  (Pa), applied on the filtration area  $A$  (m<sup>2</sup>).  $R$  (1/m) is the average resistance of the filter medium.

However, in practice, neither the solidosity nor the specific cake resistance is constant inside the filter cake so typically an average value,  $\alpha_{av}$ , is determined.

The compressibility index,  $n$ , is a commonly-used indicator of the susceptibility of the cake to compression. If  $n > 0$ , the average specific cake resistance increases with the applied pressure. A convenient method for determining  $n$  is to plot  $\alpha_{av}$  against  $\Delta p$  and to add a power-type trendline. The function is of the form (Eq. (2))

$$\alpha_{av} = \alpha_0 \Delta p^n \quad (2)$$

where  $\alpha_0$  is the average specific cake resistance at unit applied pressure.

The average porosity of a filter cake,  $\varepsilon_{av}$ , is calculated from

$$\varepsilon_{av} = \frac{V_{pores}}{V_{cake}} = 1 - \frac{V_{solids}}{V_{cake}} \quad (3)$$

where  $V$  is the volume. In this study, the volume of each filter cake was calculated based on the height (average of 5 points) and the cross-sectional area of the cake. The volumes of solids were calculated using the dry cake weights and solid densities determined earlier.

The cake compressibility has also an influence on the average porosity  $\varepsilon_{av}$ :

$$\varepsilon_{av} = \varepsilon_0 \Delta p^{-\lambda} \quad (4)$$

where  $\varepsilon_0$  is the average porosity of a filter cake at unit applied pressure and  $\lambda$  is the cake compressibility index.

The effect of mixing on the average specific cake resistance was evaluated with respect to 1) the mixing rate and 2) the mixer head, i.e. the shear pressure  $\Delta p_{shear}$ , which was calculated<sup>34</sup> from:

$$\Delta p_{shear} = \frac{P}{Q} \quad (5)$$

where  $P$  is the mixing power (W) and  $Q$  is the volumetric flow rate (m<sup>3</sup>/s).

The mixing power was estimated based on impeller power number, impeller diameter and impeller speed. The volumetric flow rate by mixer was estimated based on impeller flow number, impeller diameter and impeller speed.<sup>34</sup>

## RESULTS AND DISCUSSION

### Fiber and particle size during enzymatic hydrolysis

Enzymatic hydrolysis of cellulose and hemicellulose cleaves the polymeric structure to smaller structural units (mono-, di- and oligosaccharides). At mild conditions, for example pH 5 and at 46 °C, the solubility of lignin in the hydrolysate is low. As a result of such optimal conditions during the hydrolysis stage, it can be expected that the decrease in the fiber size of the biomass is significant. Fig. 2A shows the glucose and xylose concentrations, measured by HPLC, from the samples taken during the hydrolysis. The final glucose concentration was 39.5 g/L, which corresponds to a yield of 59 % (based on glucose only). The xylose concentration at various points during the hydrolysis was about 33 % of the glucose concentration.



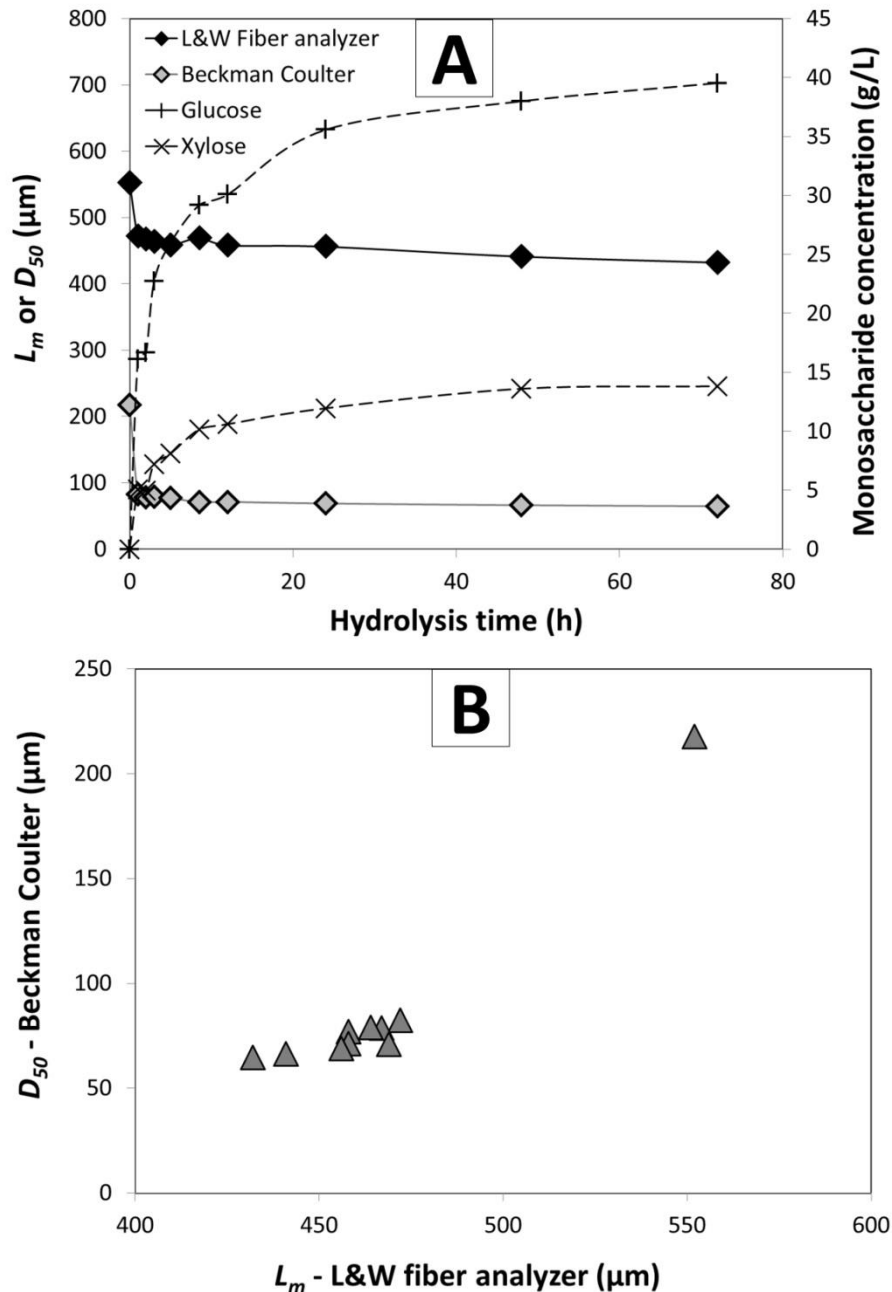


Figure 2: A) The mean fiber length ( $L_m$ ) and the median particle size ( $D_{50}$ ) of the solids, determined with an L&W fiber size analyzer and a Beckman Coulter particle size analyzer during the enzymatic hydrolysis. The corresponding concentrations of glucose and xylose in the liquid phase are also shown. B) Correlation between the mean length of fiber and the median particle size measured with the two analyzers

It is normal that the initial rate of enzymatic hydrolysis is rapid. The importance of the initial period is also observed in Fig. 2A which presents the mean fiber ( $L_m$ ) and median particle ( $D_{50}$ ) sizes. When determining fiber length, the arithmetic average fiber length was not the most suitable indicator, because of the high proportion of short fibers. Therefore, the length weighted average fiber length  $L_m$  was used. The median particle sizes ( $D_{50}$ ) were determined from volumetric particle size distributions. An approximate correlation between the measured  $L_m$  and  $D_{50}$  sizes is presented in Fig. 2B. The most probable reason for the nonlinear shape of the 2<sup>nd</sup> order fit is that the proportion of fines increases immediately after the start of hydrolysis. The

laser diffraction analyzer is able to include these fine particles in the PSD, because they are within its range of measurement. If the non-hydrolyzed sample was excluded, the correlation presented in Fig. 2B would be quite linear. The relative standard deviation for 6-9 parallel analyses with the Beckman Coulter analyzer ranged from 0.9 to 2.2 %. The fiber tester also produced very consistent data, but it is not possible to accurately evaluate the deviation based on two parallel measurements. After the first 2-3 hours of hydrolysis, the particle size does not appear to decrease significantly (Fig. 2A). The increase in glucose concentration is also rather moderate after the first 12 h. It was observed, using the laser diffraction analyzer, that the measurable size of the finest 10 % was reduced by 54 % during the first 12 hours, whereas the size limit for the largest 10 % fraction was reduced more, proportionally, by 73 %. There are a few factors that could explain why the conversion rate slows down rapidly after the enzyme addition: 1) the lack of suitable adsorption sites for the enzymes, 2) end product inhibition caused by the released sugars (not very significant in this case), 3) the presence and formation of other inhibitors, and simply 4) a lack of readily degradable cellulose. The slowdown in rate of hydrolysis has been more extensively studied<sup>35,36</sup> and also modeled<sup>37-39</sup> by other authors.

The length and width distributions of the fibers during the hydrolysis are shown in Fig. 3 A-D. During enzymatic hydrolysis, the most noticeable change in fiber length takes place during the first hour (Fig. 3 A,B). However, the fiber width distributions (Fig. 3 C,D) do not clearly correlate with the degree of enzymatic conversion.

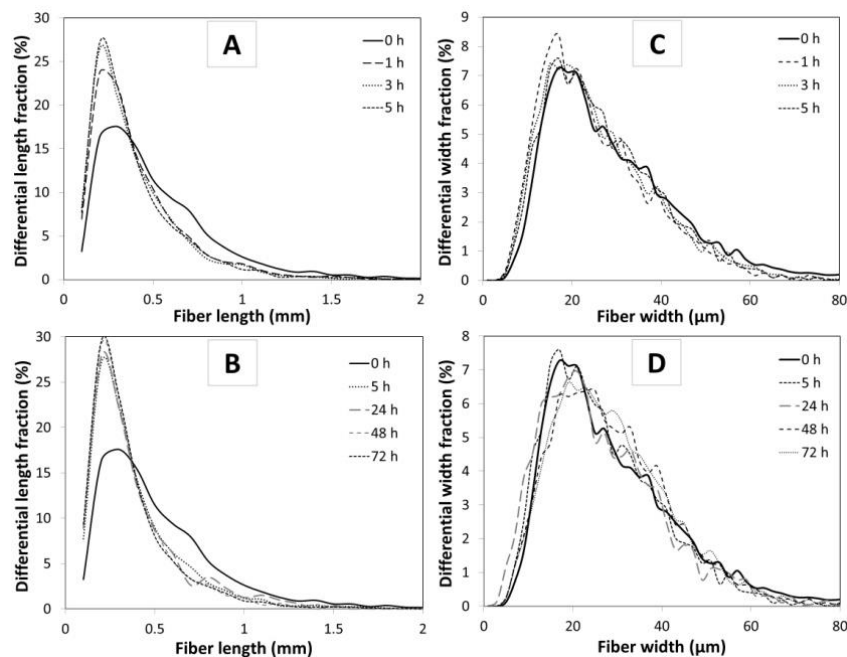


Figure 3: A) Differential fiber length distributions determined during the initial stage of hydrolysis, B) Differential fiber length distributions determined during the total course of hydrolysis, C) Differential fiber width distributions determined during the initial stage of hydrolysis, D) Differential fiber width distributions determined during the total course of hydrolysis. The distributions determined after 2, 8.5 and 12 h of hydrolysis are excluded for clarity.

The particle size distributions during the initial stages (0-5 h) and the total time of hydrolysis (72 h) are presented in Figs. 4 A-B. A comparison between Fig. 3 A-D and Fig. 4 A-B indicates that there are some similarities between the fiber and particle size distributions, even though the absolute values are not equal, as illustrated above in Fig. 2B. The particle size analyzer is

capable of accurately measuring the particle size distribution of fines, such as inorganic fillers and fragments of fibers, while fibers are more reliably characterized using the fiber tester.

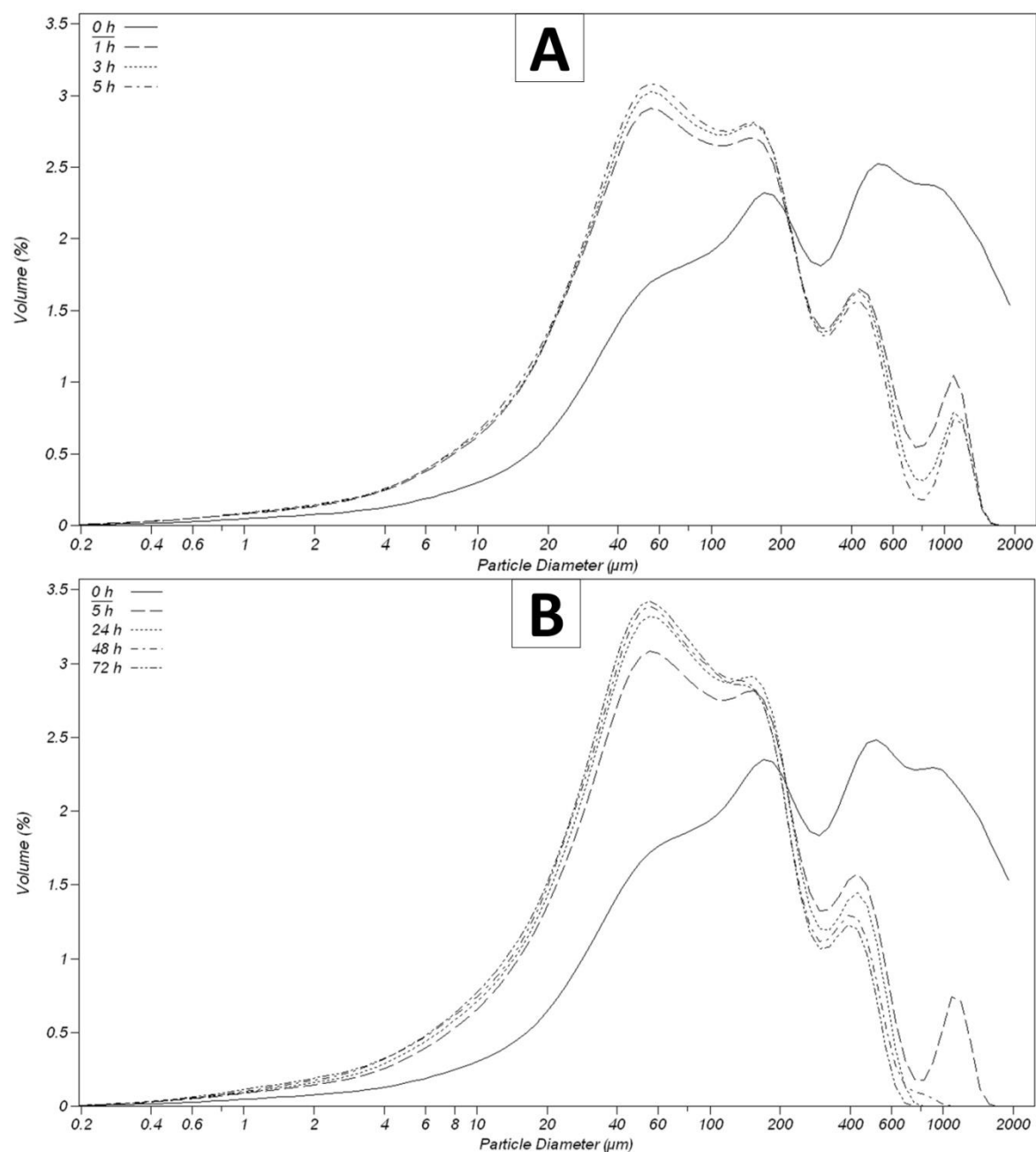


Figure 4: A) Differential particle size distributions determined during the initial stages of hydrolysis (0-5 h), B) Differential particle size distributions determined during the course of hydrolysis (72 h)

Clarke et al.<sup>40</sup> obtained a 92 % reduction in the fiber length of bleached Kraft pulp in 9 h, while a reduction of only 15 % (in 8.5 h) was obtained in this study. The negligible lignin content and the low solid loading (2 %) were probably the main reasons for such significant fiber length reduction. Mooney et al.<sup>19</sup> concluded that the role of particle size of the raw material was of the highest importance during the initial period of enzymatic hydrolysis. In their study, small fibers and fines in heterogeneous lignocellulosic substrates were cleaved to sugars rapidly, resulting

in a high hydrolysis rate at the beginning of hydrolysis. According to Zhu et al.<sup>41</sup>, the fines are hydrolyzed first and the large particles can therefore retain their original size for many hours of hydrolysis. The experimental results presented in Figs. 2-4 are unable to confirm whether similar effects occurred in this study, although it is likely that fine fibers were hydrolyzed more rapidly, because of their large specific surface area.

Fig. 5 illustrates how the structure of the fiber network changes during the hydrolysis. Because the images have been taken after the fibers have been dried, evaluation of the exact dimensions of single fibers in their suspended state is not possible. However, it is possible to evaluate approximately the size and outer structure of the fibers. This type of general evaluation supports the results that were obtained from the fiber and particle size analyses.

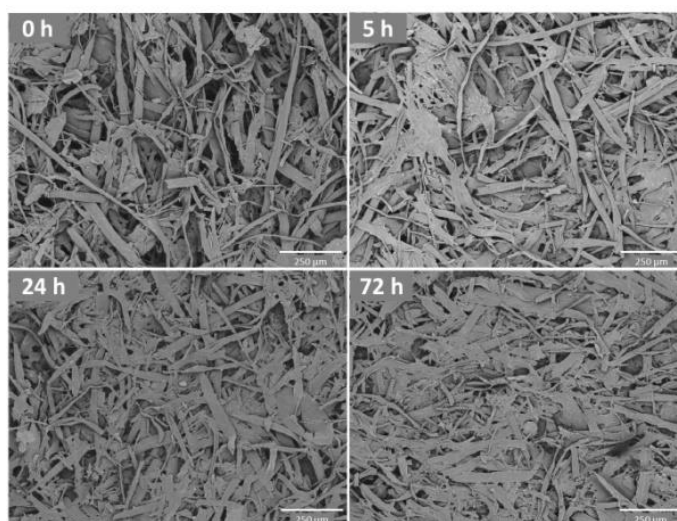


Figure 5: Scanning electron microscope (SEM) images of the fiber residue taken during the hydrolysis

Little dramatic breakage of fibers was seen, unlike that observed in the study of Clarke et al.<sup>40</sup>. Although, in each individual fiber, both the porosity and the specific surface area are likely to increase during the course of hydrolysis, the overall porosity of a dried sample seems to decrease as the saccharification proceeds. In other words, the fiber network seems to become more densely packed as a result of degradation of cellulose and hemicellulose that support the fibers. This phenomenon may also have an influence on the subsequent solid-liquid separation.

### Particle size during mixing

During mixing of the hydrolyzed suspensions at rotation speeds of 100 and 500 rpm (1.67 and 8.33 1/s), the particle sizes of the solids in the suspensions did not change dramatically. The fiber size distributions for these agitated samples were not measured, because the initial assumption was that measurement of fine particles and cut fibers would be more important. It was surprising how small the effect on particle size was, even though high-intensity mixing with the Rushton turbine continued for 4 h (Fig. 6A). In comparison with the propeller (Fig. 6B), the Rushton turbine had a stronger influence on the measured particle size. The data in Figs. 6A and 6B are presented showing the particle sizes (D10 – D90) of the undersize distribution: 10 % - 90 % of particles, on a volumetric basis, were smaller than the particle size in question. Generally, the data collected during the hydrolysis stage (Fig. 2A-B) and the results presented in Fig. 6A-B imply that omitting the fiber size analyses at this stage was reasonable.

The differences between the effect of high (500 rpm) and low (100 rpm) rotational speeds were clear only in the case of the Rushton turbine (Fig. 6A). In the case of high-speed mixing (500 rpm) with the Rushton turbine, the  $D_{10}$  and  $D_{90}$  particle sizes were decreased by 21 and 16 % during the mixing time of 4 hours. Generally, the size limit of the smallest ( $D_{10}$ ) fraction was reduced relatively more than that of the largest ( $D_{90}$ ) fraction.

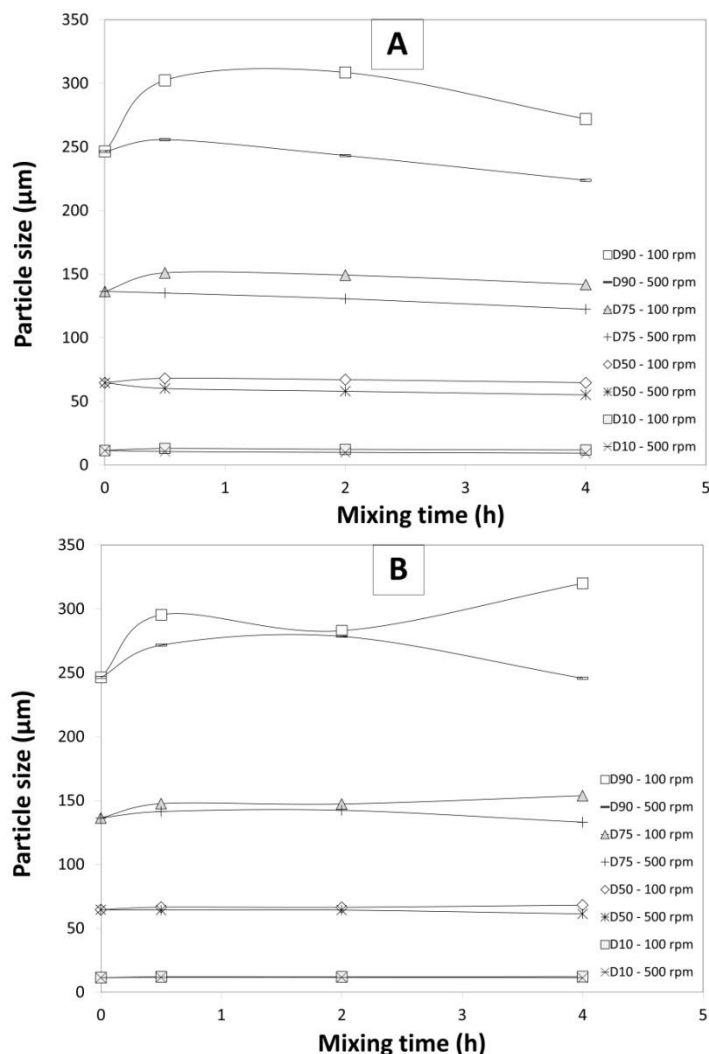


Figure 6: Particle size of hydrolyzed solids before and during agitation (0.5, 2, 4 h), at different agitation rates (100 and 500 rpm), obtained from the particle undersize distributions. A) Rushton turbine and B) Propeller

However, the use of the propeller did not lead to such notable differences in the measured particle size. It is probable that there is a relatively high degree of uncertainty in the  $D_{90}$  curves, because of the low number of particles in the largest decile. This is the most likely explanation for why, in Fig. 6B, the  $D_{90}$  particle size seems to get larger when the mixing is continued after sampling at 2 h. Other reasons for the increasing particle sizes could be presence of air bubbles in the analyzer and inaccuracy resulting from sampling and sample preparation. This could be explained by an increase in the fiber width (and volume) as a result of low-intensity mixing that is, however, unable to reduce the fiber length.

### Filtration characteristics after mixing

#### *Average specific cake resistance*

In traditional applications, where the properties of wood fibers are tailored, for instance, in the pulp and paper industry, mechanical treatment by pulping, classification, pumping, etc. may change the properties of the fibers.<sup>42,9</sup> The main changes include the dimensions, as well as physical properties. These changes can greatly affect the filtration properties of the fibers. The ability of the fibers to retain water, to swell and to be compressed under pressure is among the most important properties influenced by mixing. The average specific cake resistance is a scalable measure of the ability of a filter cake to drag the flow of liquid that passes through its pores. In practice, high average specific cake resistance signifies difficult filtration that is observed as a low filtration flow rate per unit area. Prediction of the average specific cake resistance of heterogeneous and compressible fiber suspensions based on the fiber size is problematic, because many other factors should also be taken into account. The difficulties are related to the non-uniform particle size, shape, flexibility, presence of fines, and many other factors, which affect the pore structure of the cake.<sup>43,44</sup> It is, therefore, not reasonable to predict the filtration properties based on particle size data.

In this study, the aim was to investigate how significant the effect of mixing is on the pressure filtration of enzymatically hydrolyzed suspensions. An increase in the mixing rate, i.e. the local shear rate, resulted in considerably elevated average specific cake resistances (Fig. 7).

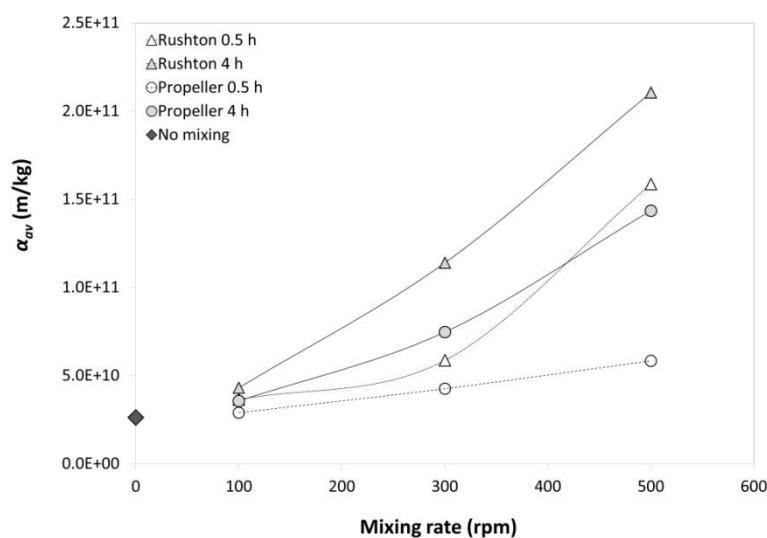


Figure 7: Average specific cake resistances obtained by pressure filtration experiments after 0.5 and 4 hours of mixing with the Rushton turbine and the traditional propeller at three different mixing rates. The zero mixing value is shown for comparison

This was especially clear in the case of the Rushton turbine. However, the particle size data do not support the assumption that this was the result of a significant decrease in the fiber size. The most important conclusion from this is that the fiber properties, which could not be directly measured, such as an increase in the number of microfibrils and other structural changes in the fiber, increase  $\alpha_{av}$ . Partial fibrillation of the fibers is likely to be one main reason for the increased resistance to filtration. This explanation is analogous to drainage of non-hydrolyzed wood fibers on a paper machine, where excessive fibrillation of fibers should be avoided, in order to obtain a good drainage rate. However, fibrillation cannot be observed in the SEM images prepared using dry fibers. Another interesting point is the behavior of lignin in the process. Lignin was almost exclusively in the solid state at the filtration conditions (pH 5, 23 °C) and may have also been affected by agitation. In comparison with inorganic fines, small lignin particles are typically more difficult to be separated by cake filtration. At the process pH,

most of the lignin was in the solid state, attached to the carbohydrate polymers in the fibers. Quantification of the amount of free lignin-rich particles in the suspension would have been interesting but technically challenging.

The average specific cake resistances shown in Fig. 7 are presented as a function of the mixer head in Fig. 8A (Rushton turbine) and 8B (propeller). The mixer head, calculated from Eq. (5), corresponds to shear pressure (Pa) produced by the impeller.

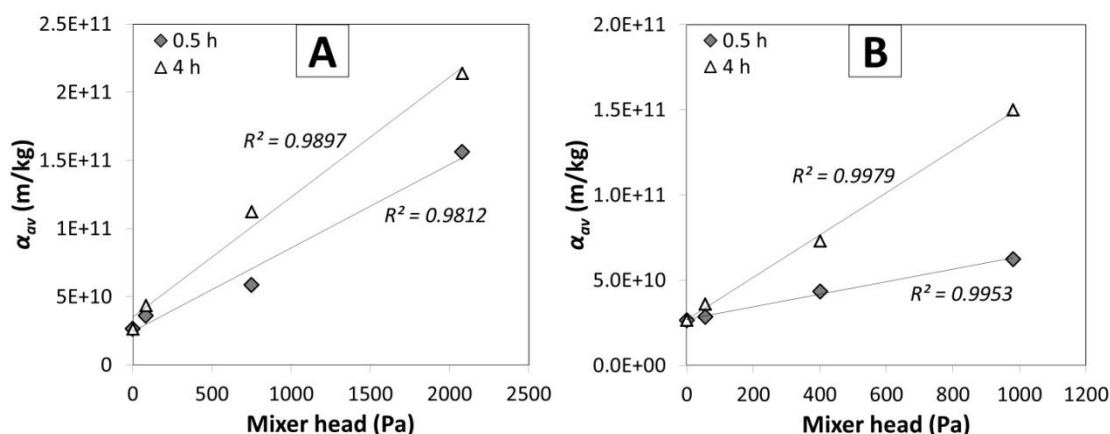


Figure 8: Average specific cake resistances obtained by pressure filtration experiments after 0.5 and 4 hours of mixing at different shear pressures (the zero mixing value is also shown). A) Rushton turbine and B) Propeller

It was observed that the filtration performance depends on the mixing time and shear pressure. The correlation between shear pressure and filtration performance is linear. The linear fit for the data was good ( $R^2 = 0.981 - 0.998$ ). The results presented in Figs. 7 and 8 illustrate the importance of the mixer geometry with respect to solid-liquid separation. It is apparent that the results obtained using the Rushton turbine and the propeller are more comparable when the influence of mixing geometry is taken into account, in addition to the mixing rate.

### ***Cake compressibility and porosity***

Determination of the cake compressibility index  $n$  for the non-mixed and the strongly mixed (Rushton turbine, 4 h, 500 rpm) hydrolyzed suspensions was performed by plotting the average specific cake resistance,  $\alpha_{av}$ , against the filtration pressure (Fig. 9A). The exponent in the power function fitted to the data represents the compressibility index. The more sharply  $\alpha_{av}$  increases with pressure the more compressible is the filtered material. In spite of the high average specific cake resistance in the separation of the mixed suspension and even though, in this case, the cake resistance was strongly affected by the filtration pressure, the compressibility index did not increase greatly as a result of mixing.

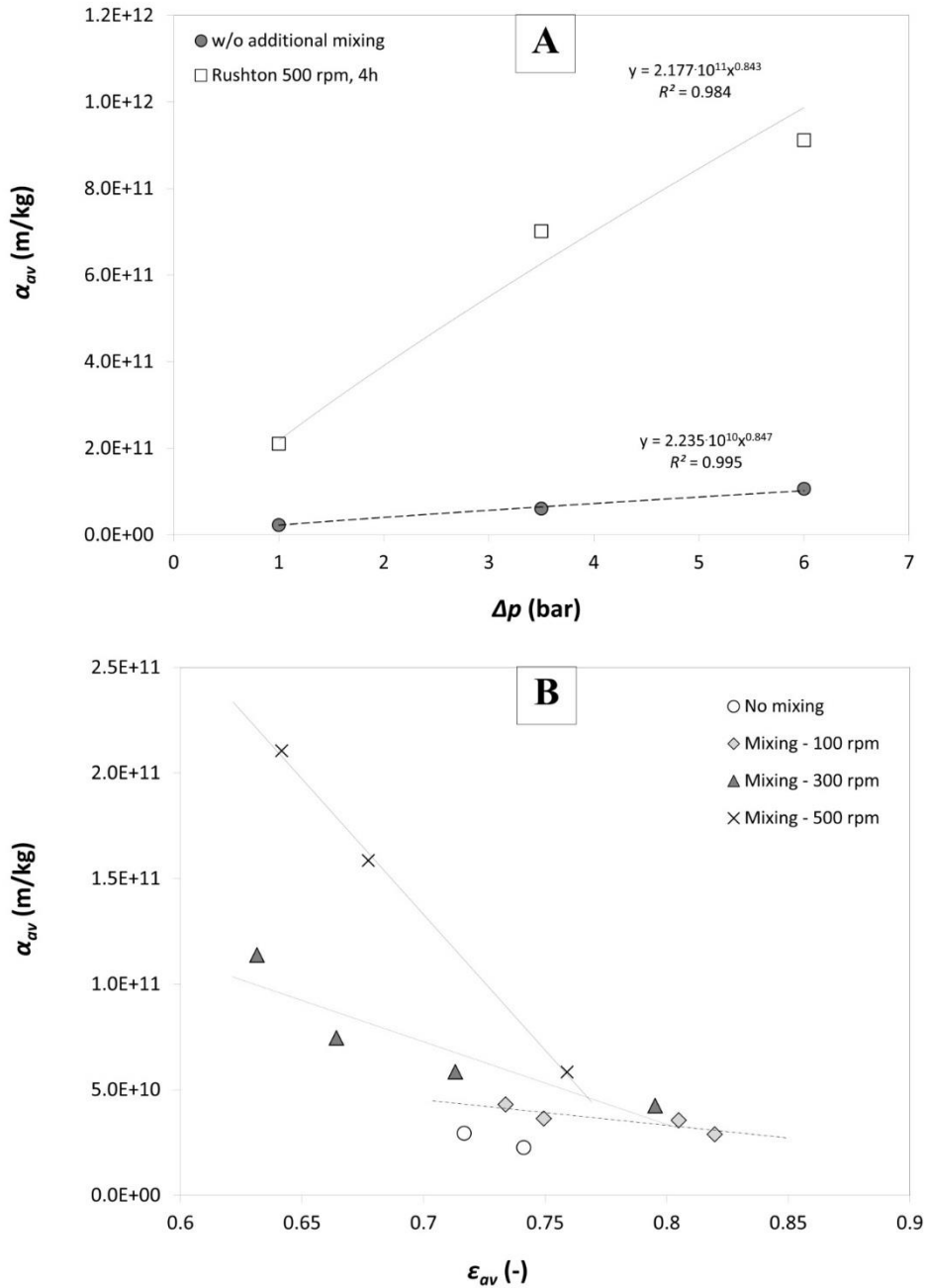


Figure 9: A) Dependence of the average specific cake resistance on the filtration pressure ( $\Delta p$ ). The pressure filtration experiments were performed immediately after hydrolysis and after 4 hours of mixing with the Rushton turbine at 500 rpm. B) The average cake porosity and its relationship with the average specific cake resistance, obtained at different mixing rates

The compressibility indices  $n$  for the cakes obtained for the mixed and non-mixed suspensions were 0.84 and 0.85, respectively. In the case of dewatering of wastewater sludge, the separation is even more difficult: the compressibility index is typically 1-2, sometimes higher,<sup>45</sup> and the compressive pressure does not always affect the filtration rate.<sup>46</sup>

Mixing not only increased the cake resistance but also resulted in a simultaneous reduction in the cake porosity (Fig. 9B). It is clear that mixing speed had a major effect on both the porosity



and the average specific cake resistance. The pretreatment and the enzymatic hydrolysis are generally thought to increase the porosity<sup>8</sup> of fibers and vice versa.<sup>47</sup> However, such well-hydrolyzed fibers are more susceptible to mechanical compression in a pressure filter, which leads to a decrease in the cake porosity and an increase in the average specific cake resistance.<sup>48</sup> This is also somewhat analogous to sludge dewatering, where the organic matter has been partly decomposed and the resulting cakes are viscoelastic, highly compressible and cause a high cake resistance.<sup>46</sup> The partial breakdown of the fiber network in the filter cake, as well as the apparent increase in the fibrillation of fibers, which take place while the suspension is mixed intensively, have a similar effect on the cake properties. The validity of the above speculations could be evaluated using more representative sample imaging techniques, preferably for wet fibers. Additionally, it would probably be useful to analyze the solids further in order to evaluate changes in the specific surface area and shape of the fibers and other particles.

### Regression model with combined effect of mixing rate and time

Both mixing rate and time had an influence on the average specific cake resistance and the average porosity. The process was investigated employing a linear regression model supplemented with the combined effect of the variables (Eq. (6)):

$$y = \beta_0 + \beta_1 X1 + \beta_2 X2 + \beta_3 X1X2 \quad (6)$$

where  $X1$  is the coded value of the rotation speed of the impeller (rpm) and  $X2$  is the coded value of the mixing time (h). The coded values of variables ranged from -1, which corresponded to the minimum value of the variable, to 1 that represented the maximum. The dimensionless coefficients  $\beta_0 - \beta_3$  were determined (Table 2).

Table 2  
Dimensionless coefficients  $\beta_0 - \beta_3$  for each regression model

Mixer type	Characteristic	$R^2$	$\beta_1$	$\beta_2$	$\beta_3$	$\beta_0$
Rushton	$\alpha_{av}$	0.955	$7.238 \cdot 10^{10}$	$1.899 \cdot 10^{10}$	$1.133 \cdot 10^{10}$	$1.035 \cdot 10^{11}$
	$\varepsilon_{av}$	0.982	$-9.205 \cdot 10^{-2}$	$-5.616 \cdot 10^{-2}$	$-5.600 \cdot 10^{-2}$	$6.571 \cdot 10^{-1}$
Propeller	$\alpha_{av}$	0.983	$3.432 \cdot 10^{10}$	$2.064 \cdot 10^{10}$	$1.964 \cdot 10^{10}$	$6.391 \cdot 10^{10}$
	$\varepsilon_{av}$	0.965	$-6.393 \cdot 10^{-2}$	$-4.915 \cdot 10^{-2}$	$-3.357 \cdot 10^{-2}$	$7.422 \cdot 10^{-1}$

The coefficients of determination  $R^2$  for all models were good. It is possible to obtain estimates for  $\alpha_{av}$  and  $\varepsilon_{av}$  using Eq. (6), coefficients  $\beta_0 - \beta_3$  and the coded values of the variables. In this case, the inclusion of the combined effect of mixing rate and time improved the correlation: for instance, the  $R^2$  values for  $\alpha_{av}$  in the case of Rushton turbine and propeller were improved from 0.93 to 0.96 and from 0.81 to 0.98, respectively.

The modeled and measured values for  $\alpha_{av}$  and  $\varepsilon_{av}$ , obtained using both types of mixer, are shown in Fig. 10A-B. The agreement between the modeled values and those measured is good.

However, the use of Rushton turbine seems to have resulted in an increased divergence between the measured and modeled  $\alpha_{av}$ , although it is difficult to identify a reason for this effect. More generally, the main reason for the good accuracy of the model is that the effect of chemical phenomena, such as those taking place during the pretreatment and hydrolysis stages, were excluded by using the same batch of slurry in the mixing experiments.

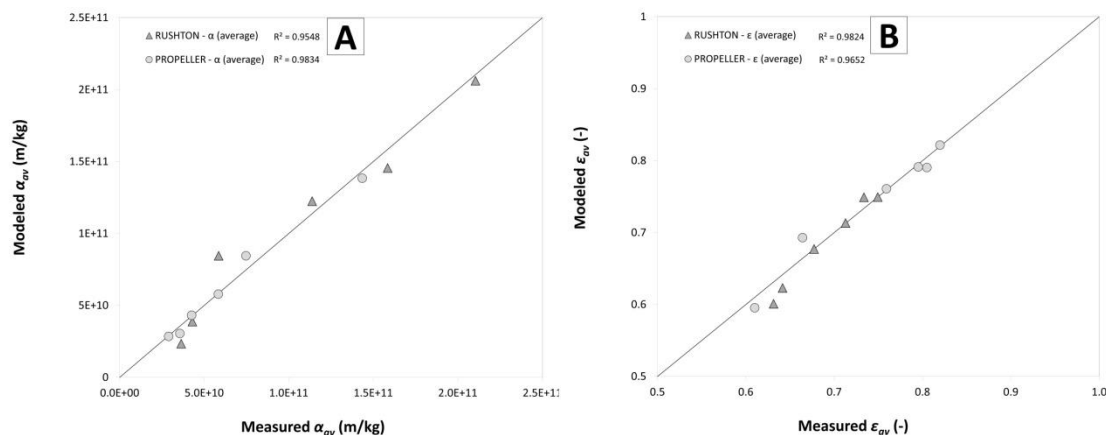


Figure 10: Measured and modeled values for A) the average specific cake resistances  $\alpha_{av}$  and B) the average porosities of the filter cakes  $\epsilon_{av}$

## CONCLUSION

In this study, the filtration properties of hydrolyzed and agitated biomass suspensions were determined using a pressure filter. It was shown that upstream process conditions have a pivotal role in the solid-liquid separation of a lignocellulosic hydrolysate. The average specific cake resistance increased linearly with the shear pressure caused by mixing. Intensive mixing and pumping of hydrolyzed suspensions should, therefore, be avoided. However, the success in the separation stage should not be predicted based solely on the fiber or particle size data. It is apparent that advanced analysis techniques are necessary in order to better understand the micro- and nano-scale changes that take place in the fibers and that consequently affect the cake filtration characteristics. These techniques include, in particular, 1) nano-scale imaging of the wet solids and 2) thorough investigation of the electrochemical phenomena and interactions.

## REFERENCES

- <sup>1</sup> L. Viikari, J. Vehmaanperä and A. Koivula, *Biomass Bioenerg.*, 46, 13 (2012).
- <sup>2</sup> J. Larsen, M. Østerhgaard Haven and L. Thirup, *Biomass Bioenerg.*, 46, 36 (2012).
- <sup>3</sup> K. Kemppainen, L. Ranta, E. Sipilä, A. Östman, J. Vehmaanperä, T. Puranen, K. Langfelder, J. Hannula, A. Kallioinen, M. Siika-aho, K. Sipilä and N. von Weymarn, *Biomass Bioenerg.*, 46, 60 (2012).
- <sup>4</sup> L. Wang, R. Templer and R.J. Murphy, *Appl. Energ.*, 99, 23 (2012).
- <sup>5</sup> M. Mandels, L. Hontz and J. Nystrom, *Biotechnol. Bioeng.*, XVI, 1471 (1974).
- <sup>6</sup> J.I. Walpot, *Conserv. Recycl.*, 9(1), 127 (1986).

- <sup>7</sup> M.M. Nazhad, L.P. Ramos, L. Paszner and J.N. Saddler, *Enzyme Microb. Tech.*, 17, 68 (1995).
- <sup>8</sup> S.D. Mansfield, C. Mooney and J.N. Saddler, *Biotechnol. Progr.*, 15, 804 (1999).
- <sup>9</sup> X. Luo, J.Y. Zhu, *Enzyme Microb. Tech.*, 48, 92 (2011).
- <sup>10</sup> T. Kinnarinen, M. Huhtanen, A. Häkkinen and M. Louhi-Kultanen, *Ind. Crop. Prod.*, 38(1), 72 (2012).
- <sup>11</sup> M. Balat, H. Balat and C. Öz, *Prog. Energ. Combust.*, 34, 551 (2008).
- <sup>12</sup> D.R. Burke, J. Anderson, P.C. Gilcrease and T.J. Menkhaus, *Biomass Bioenerg.*, 35, 391 (2011).
- <sup>13</sup> I. Virkajärvi, M. Veringa Niemelä, A. Hasanen and A. Teir, *BioResources*, 4(4), 1718 (2009).
- <sup>14</sup> B. Hahn-Hägerdal, M. Galbe, M.F. Gorwa-Grauslund, G. Lidén and G. Zacchi, *Trends Biotechnol.*, 24, 549 (2006).
- <sup>15</sup> P. Sassner, M. Galbe and G. Zacchi, *Biomass Bioenerg.*, 32, 422 (2008).
- <sup>16</sup> Y. Qi, K.B. Thapa and A.F.A. Hoadley, *Chem. Eng. J.*, 171, 373 (2011).
- <sup>17</sup> L. Mäkinen, A. Ämmälä, M. Körkkö and J. Niinimäki, *Resour. Conserv. Recycl.*, 73, 11 (2013).
- <sup>18</sup> S. Al-Zuhair, *Bioresource Technol.*, 99, 4078 (2008).
- <sup>19</sup> C.A. Mooney, S.D. Mansfield, R.P. Beatson and J.N. Saddler, *Enzyme Microb. Tech.*, 25, 644 (1999).
- <sup>20</sup> S.D. Mansfield, E. de Jong, R.S. Stephens and J.N. Saddler, *J. Biotechnol.*, 57, 205 (1997).
- <sup>21</sup> L. Del Rio, R.P. Chandra and J.N. Saddler, *Bioresource Technol.*, 107, 235 (2012).
- <sup>22</sup> A. Yeh, Y. Huang and S.H. Chen, *Carbohydr. Polym.*, 79, 192 (2010).
- <sup>23</sup> I. Spiridon, A.P. Duarte and M.N. Belgacem, *Appita J.*, 54(5), 457 (2001).
- <sup>24</sup> R.P. Chandra, R. Bura, W.E. Mabee, A. Berlin, X. Pan and J.N. Saddler, *Adv. Biochem. Eng. Biot.*, 108, 67 (2007).
- <sup>25</sup> L. Wang, Y. Zhang, P. Gao, D. Shi, H. Liu and H. Gao, *Biotechnol. Bioeng.*, 93(3), 443 (2005).
- <sup>26</sup> G. Chinga-Carrasco, P.O. Johnsen and K. Oyaas, *Micron*, 41, 648 (2010).
- <sup>27</sup> H. Liu, S. Fu, J.Y. Zhu, H. Li and H. Zhan, *Enzyme Microb. Tech.*, 45, 274 (2009).

- <sup>28</sup> D.M. Lavenson, E.J. Tozzi, N. Karuna, T. Jeoh, R.L. Powell, *Bioresource Technol.*, 111, 240 (2012).
- <sup>29</sup> D. Taneda, Y. Ueno, M. Ikeo, S. Okino, *Bioresource Technol.*, 121, 154 (2012).
- <sup>30</sup> T. Kinnarinen, M. Shakhanova, E. Hietanen, R. Salmimies, A. Häkkinen and M. Louhi-Kultanen, *Bioresource Technol.*, 110(1), 405 (2012).
- <sup>31</sup> J.S. Van Dyk and B.I. Pletsche, *Biotechnol. Adv.*, 30(6), 1458 (2012).
- <sup>32</sup> D. Cannella, C.C. Hsieh, C. Felby and H. Jorgensen, *Biotechnol. Biofuels*, 5:26 (2012).
- <sup>33</sup> I.C. Hoeger, S.S. Nair, A.J. Ragauskas, Y. Deng, O.J. Rojas and J.Y. Zhu, *Cellulose*, 20(2), 807 (2013).
- <sup>34</sup> R.R. Hemrajani, G.B. Tatterson, In: *Handbook of Industrial Mixing*, Eds.: E.L. Paul, V.A. Atiemo-Obeng, S.M. Kresta. John Wiley & Sons, Inc., Hoboken, New Jersey.
- <sup>35</sup> Q. Gan, S.J. Allen and G. Taylor, *Process Biochem.*, 38, 1003 (2003).
- <sup>36</sup> B. Yang, D.M. Willies and C.E. Wyman, *Biotechnol. Bioeng.*, 94, 1122 (2006).
- <sup>37</sup> K. Movagarnejad, M. Sohrabi, T. Kaghazchi and F. Vahabzadeh, *Biochem. Eng. J.*, 4, 197 (2000).
- <sup>38</sup> K. Movagarnejad and M. Sohrabi, *Biochem. Eng. J.*, 14, 1 (2003).
- <sup>39</sup> K. Movagarnejad, *Biochem. Eng. J.*, 24, 217 (2005).
- <sup>40</sup> K. Clarke, X. Li and K. Li, *Biomass Bioenerg.*, 35, 3943 (2011).
- <sup>41</sup> J.Y. Zhu, G.S. Wang, X.J. Pan and R. Gleisner, *Chem. Eng. Sci.*, 64, 474 (2009).
- <sup>42</sup> M.A. Hubbe, R.A. Venditti and O.A. Rojas, *BioResources*, 2(4), 739 (2007).
- <sup>43</sup> H. Liimatainen, *Interactions between fibres, fines and fillers in papermaking*. Ph.D. Thesis, University of Oulu, Finland (2009).
- <sup>44</sup> K.-J. Hwang, Y.-S. Wu, W.-M. Lu, *Powder Technol.*, 87, 161 (1996).
- <sup>45</sup> R.M. Wu, D.J. Lee, C.H. Wang, J.P. Chen and R.B.H. Tan, *Wat. Res.*, 35(5), 1358 (2001).
- <sup>46</sup> D.J. Lee and C.H. Wang, *Wat. Res.*, 34(1), 1 (2000).
- <sup>47</sup> V. Arantes and J.N. Saddler, *Biotechnol. Biofuels*, 4, 1 (2011).
- <sup>48</sup> T. Kinnarinen and A. Häkkinen, Filtration characteristics of enzymatically hydrolyzed and fermented biomass suspensions, in Proceedings of the 20th European Biomass Conference and Exhibition, Milan, June 18 – 22, 2012.